Contents lists available at ScienceDirect

Remote Sensing of Environment

A spectral analysis of common boreal ground lichen species

Nea Kuusinen[a],[*], Jussi Juola[a], Bijay Karki[a], Soili Stenroos[b], Miina Rautiainen[a],[c]

[a] Department of Built Environment, School of Engineering, Aalto University, P.O. Box 14100, FI-00076 Aalto, Finland
[b] Botany Unit, Finnish Museum of Natural History, P.O. Box 7, FI-00014, University of Helsinki, Finland
[c] Department of Electronics and Nanoengineering, School of Electrical Engineering, Aalto University, P.O. Box 15500, 00076 Aalto, Finland

ARTICLE INFO

ABSTRACT

Lichens dominate a significant part of the Earth's land surface, and are valuable bioindicators of various environmental changes. In the northern hemisphere, the largest lichen biomass is in the woodlands and heathlands of the boreal zone and in tundra. Despite the global coverage of lichens, there has been only limited research on their spectral properties in the context of remote sensing of the environment. In this paper, we report spectral properties of 12 common boreal lichen species. Measurements of reflectance spectra were made in laboratory conditions with a standard spectrometer (350–2500 nm) and a novel mobile hyperspectral camera (400–1000 nm) which was used in a multiangular setting. Our results show that interspecific differences in reflectance spectra were the most pronounced in the ultraviolet and visible spectral range, and that dry samples always had higher reflectance than fresh (moist) samples in the shortwave infrared region. All study species had higher reflectance in the backward scattering direction compared to nadir or forward scattering directions. Our results also reveal, for the first time, that there is large intraspecific variation in reflectance of lichen species. This emphasizes the importance of measuring several replicates of each species when analyzing lichen spectra. In addition, we used the data in a spectral clustering analysis to study the spectral similarity between samples and species, and how these similarities could be linked to different physical traits or phylogenetic closeness of the species. Overall, our results suggest that spectra of some lichen species with large ground coverage can be used for species identification from high spatial resolution remote sensing imagery. On the other hand, for lichen species growing as small assemblages, mobile hyperspectral cameras may offer a solution for in-situ species identification. The spectral library collected in this study is available in the SPECCHIO Spectral Information System.

1. Introduction

Lichens are symbiotic life forms, based on associations between a mycobiont (fungus) and a photobiont (alga or/and cyanobacterium). There are about 17,500–20,000 lichen species on Earth (Stenroos, 2011). Lichens occur in numerous different regions, but are the most abundant in cold and nutrient-poor high latitude or altitude areas, where they may occur as dominant ground layer species (Asplund and Wardle, 2017). Despite their global ground coverage and potential importance in radiative forcing in cold regions, there have been no systematic efforts to publish spectral libraries of lichens or to analyze their spectral differences in larger extent. Hyperspectral measurement techniques, using spectrometers mounted on drones or aircraft, may offer a new approach to mapping and monitoring lichen species diversity.

Lichens are slow-growing organisms that occur typically on soil, humus, tree trunks and on rock and stones. They cover a vast range of physical and functional traits, related to associations with symbionts, water and nutrient uptake and retention, growth form, specific thallus mass, color, and secondary compounds (Asplund and Wardle, 2017). They have no root system, and take up water and nutrients directly from rainfall and wet and dry deposition and may consequently affect the growth of vascular plants through their influence on soil nutrient and moisture content (Asplund and Wardle, 2017). The uptake of elements from dry deposition also makes most lichen species susceptible to air pollution, particularly sulfuric acid (Nash, 2008).

Due to their susceptibility to environmental changes, lichens can serve as valuable bioindicators of these changes. An increase in nitrogen deposition has been observed to have a negative effect on many lichen species (Bobbink et al., 2010), and the increase in air temperature in the Arctic tundra has been thought to reduce lichen growth through growth and shading of higher vascular plants (Elmendorf et al.,

Table 1
Number of samples in spectral measurements by species. The nadir measurements were conducted with a spectrometer and multiangular measurements with a hyperspectral camera (see Section 2.2.)

Species	Nadir measurements		Multiangular measurements	
	N of samples	Sample size	N of samples	Sample size
Cetraria islandica subsp. *islandica*	10	250 cm^2	3	250 cm^2
Cladonia arbuscula subsp. *squarrosa*	10	250 cm^2	3	250 cm^2
Cladonia rangiferina	10	250 cm^2	3	250 cm^2
Cladonia stellaris	10	250 cm^2	3	250 cm^2
Cladonia uncialis subsp. *uncialis*	10	250 cm^2	3	250 cm^2
Stereocaulon tomentosum	8	250 cm^2	3	250 cm^2
Stereocaulon saxatile	4	50 cm^2	–	–
Cladonia cornuta subsp. *cornuta*	4	50 cm^2	–	–
Cladonia crispata var. *crispata*	4	50 cm^2	–	–
Cladonia gracilis subsp. *gracilis*	3	50 cm^2	–	–
Cladonia gracilis subsp. *turbinata*	5	50 cm^2	–	–
Cladonia phyllophora	5	50 cm^2	–	–

2012). However, for example in Finland, the main threat to lichen diversity is currently the loss of habitats due to forest management, and to a lesser extent, also mining and construction activities (Jääskeläinen, 2011). Lichen cover in the northern areas is influenced by reindeer and caribou grazing, and, thus, several studies have estimated lichen cover in reindeer pasture areas from satellite data (e.g. Käyhkö and Pellikka, 1994; Nordberg and Allard, 2002; Nelson et al., 2013; Falldorf et al., 2014). Grazing can have several environmental effects; Stoy et al. (2012) observed a decrease in surface albedo in *Cladonia* dominated areas affected by reindeer grazing compared to relatively undisturbed areas.

Lichens differ widely in their structure and pigmentation, but already early studies on ground lichen spectra have shown that they deviate from spectra of other surface types such as vegetation and soil (Petzold and Goward, 1988). Generally, lichens exhibit a higher visible reflectance and a more gradual increase of reflectance from red to near-infrared than green vegetation (Petzold and Goward, 1988; Rees et al., 2004; Peltoniemi et al., 2005). However, as an exception to this, Petzold and Goward (1988) found the dark pigmented *Cetraria ericetorum* to have a very low reflectance in visible wavelengths. Another typical feature of lichens' spectra observed in laboratory and in-situ measurements is strong backward scattering (reflectance in illumination direction) (Solheim et al., 2000; Kaasalainen and Rautiainen, 2005; Peltoniemi et al., 2005). In addition, moisture content has been observed to affect lichen spectra particularly in the shortwave infrared region (Granlund et al., 2018).

Distinguishable spectral features enable the detection of the presence of ground lichens from remotely sensed data, which is crucial for monitoring changes in species composition related to climate warming and changes in precipitation, pollution, and land use change such as occurring due to changes in reindeer herding. To achieve accurate information on lichen diversity from remotely sensed data, however, detailed information on variation in lichen spectra due to, e.g., intraspecific variation caused by differences in growth conditions, variation across lichen species and families, and angular distribution of reflected radiation, is required. So far, only a few studies have measured lichen spectra in-situ or in laboratory conditions (Petzold and Goward, 1988, Bechtel et al. 2002, Nordberg and Allard, 2002, Rees et al., 2004, Neta et al., 2010, Granlund et al., 2018). In no study, to our knowledge, have several samples of the same lichen species been collected to examine the intraspecific spectral variation and its causes. Systematic evaluation of the taxonomical variation in lichen spectra has also not been done. In addition, only a few studies have examined the directionality of lichen reflectance (Solheim et al., 2000; Kaasalainen and Rautiainen, 2005; Peltoniemi et al., 2005), although understanding of the directional reflectance properties of any surface is important for the interpretation of remote sensing data. Moreover, the spectral

measurements of many studies on lichens do not cover the shortwave infrared region from 1300 to 2500 nm, which has been observed to be essential in the identification of, e.g., different tree species (Hovi et al., 2017).

High and medium spatial resolution satellite data can be used to map the presence of ground lichens in an area (e.g. Käyhkö and Pellikka, 1994; Thèau et al., 2005; Nelson et al., 2013; Falldorf et al., 2014; Keim et al., 2016). However, if more detailed information on lichen diversity or the presence and abundance of a certain lichen taxon is desired, very high spatial resolution hyperspectral data collected by instruments attached to drones or aircraft may become useful. Alternatively, if mobile hyperspectral cameras become more common in environmental surveys, images acquired with them as part of field campaigns may be used to identify lichens automatically by non-experts. Lichen species are often difficult to separate visually, and hence, spectral information could provide a new means not only for remote sensing of them but also for in-situ species identification. The prerequisite for these activities is, of course, that lichen taxa are spectrally separable from each other at, e.g., genus or species level.

In the northern hemisphere, the largest lichen biomass is found in the woodlands and heathlands of the boreal zone and in tundra (Nash, 2008). In this study, we collected and published a spectral library of common boreal ground lichen species and analyzed intra- and inter-specific differences in their nadir spectra (350–2500 nm). Furthermore, we used the spectral library to study if phylogenetically closely related (Miadlikowska et al., 2014; Stenroos et al., 2019) lichen species or lichen species with similar physical traits are also spectrally related. In addition, we applied a set-up for measuring the spatial variation in lichen spectra from multiple view angles using a novel hyperspectral camera. The multiangular hyperspectral images provided, for the first time, an understanding of the detailed spatial and angular characteristics of lichen reflectance spectra.

2. Material and methods

2.1. Lichen samples

Lichen samples were collected from Pirkanmaa area (61°20′N, 24°29′E) in southern Finland in October–November 2019. All the measured species (Table 1) are very common in Finland and exist throughout the boreal zone. Most of the lichens were collected from upland forests with exposed rocks and stones, on which lichens (*Cladonia, Cetraria*) grew typically on a shallow humus layer together with mosses. The dominant tree species in these sites was Scots pine (*Pinus sylvestris*). Samples of *Stereocaulon* spp., as well as some of the *Cladonia* samples were collected from old gravel pits with sandy soil. Samples of ~250 cm^2 (about 16 cm × 16 cm) in size were removed carefully from

the ground and placed in low carton boxes with plastic on the bottom. An exception were the not mat-forming species that could only be found as small assemblages and were consequently collected as ~50 cm^2 (about 7 cm × 7 cm) sized samples (Table 1). Any tree needles, vascular plants and other lichen species were removed from the samples. After collection, the samples were transported by car for two hours to Aalto University holdings. Until the spectral measurements next day, the samples were stored outside in ambient (natural) conditions, although under a shelter, to maintain the natural moisture content. In one case, the samples had to be stored outside for two days (these samples did not stand out in the spectral analysis). During the whole measuring period, the weather was cold (−3–+8 °C) and moist.

Two types of spectral measurements were conducted (Section 2.2.), and separate lichen samples were collected for each (Table 1). For the nadir measurements with a spectrometer, the original aim was to measure ten samples per species of common mat-forming ground lichen species and five samples per species of lichens that naturally cover smaller patches of ground when present. However, when all the samples were checked by an expert (Prof. S. Stenroos) after the spectral measurements, some of the samples had to be removed because they belonged to some (usually quite rare) species with not enough samples for the analysis. For the multi-angular measurements with a hyperspectral camera, three samples of six most abundant species (Table 1) were collected and analyzed. Table 1 shows the final number and size of the samples used in the analysis. Field photographs of the sampled species as well as their full names including authorities can be found in the Appendix.

In later text, the lichen species *Cladonia arbuscula* subsp. *squarrosa* is simply called "*Cladonia arbuscula*", *Cladonia uncialis* subsp. *uncialis* "*Cladonia uncialis*", *Cetraria islandica* subsp. *islandica* "*Cetraria islandica*", *Cladonia cornuta* subsp. *cornuta* "*Cladonia cornuta*" and *Cladonia crispata* var. *crispata* "*Cladonia crispata*".

2.2. Reflectance measurements

2.2.1. Spectrometer measurements

All reflectance measurements were conducted in a dark laboratory equipped for spectral measurements. The measurement table was covered by a black cloth, and the room walls and doors were painted with black paint. We used the FieldSpec 4 spectroradiometer by Analytical Spectral Devices Inc. (ASD, serial number: 18641) to measure the nadir-view reflectance of the lichen samples. The spectral range of the device is 350–2500 nm and resolution 3 nm at 700 nm and 10 nm at 1400 and 2100 nm. The field-of-view (FOV) is 25°. The light source was a 12 V 50 W Quartz Tungsten Halogen lamp with a 36° beam. The beam was further restricted by a black-painted aluminum can to avoid stray light scattering to the sensor (Juola, 2019). The illumination zenith angle was 40°. The optical fiber was attached to a boom above the measurement table. Two different measurement heights were used: 30 cm above the sample surface for large (250 cm^2) samples and 15 cm above the sample surface for small (50 cm^2) samples, providing ground FOVs of 6.65 cm and 3.33 cm in radius, respectively. The measurement setup is illustrated in Fig. A1 in the Appendix.

The quantity measured was the *biconical reflectance factor* (Schaepman-Strub et al., 2006):

$$R = \frac{I_s - I_{dc}}{I_{wr} - I_{dc}} \times R_{wr} \tag{1}$$

where R is the biconical reflectance factor, hereafter reflectance, I_s is the spectrometer reading of the sample, I_{dc} the dark current reading, I_{wr} the spectrometer reading of the white reference panel, and R_{wr} the reflectance factor of the white reference. We used a 10-in. factory calibrated Spectralon® reference panel as the white reference.

The reflectance spectra of all lichen samples were measured twice in order to evaluate the effect of moisture on reflectance spectra. First, each sample was measured right after it was brought from outdoors to

the laboratory, i.e. with natural moisture content. Recall that lichen takes up water from the air and rainfall, which makes its moisture content dependent on the prevailing air humidity. After the first measurements, the samples were stored indoors to allow them to dry and were measured again after two days. In order to obtain a rough estimate of water loss during the two-day period, the samples were weighed as "fresh" and as "dry". The small samples (~50 cm^2) were weighted as whole, whereas from the larger samples (~250 cm^2) a ca. 12 cm^2 piece was detached from the corner of each sample for weighting. The average water loss and its standard deviation per species were: 64% and 11% for *Cladonia stellaris*, 62% and 8% for *Cladonia arbuscula*, 65% and 4% for *Cladonia rangiferina*, 56% and 5% for *Cetraria islandica*, 58% and 11% for *Cladonia uncialis*, 64% and 19% for *Stereocaulon tomentosum*, 45% and 7% for *Stereocaulon saxatile*, 38% and 8% for *Cladonia cornuta*, 51% and 11% for *Cladonia crispata*, 52% and 2% for *Cladonia gracilis* subps. *gracilis*, 51% and 8% for *Cladonia gracilis* subps. *turbinata,* 50% and 3% for *Cladonia phyllophora*. Note that the initial water content of the samples varied depending on the weather, and samples of the same species may have been collected on different days.

2.2.2. Multiangular measurements with a hyperspectral camera

Multiangular hyperspectral measurements were conducted with a Specim IQ hyperspectral camera manufactured by Spectral Imaging Ltd. attached to a goniometer arm (see Juola, 2019 for details). The Specim IQ camera provides a 400–1000 nm spectral range and a spectral resolution of 7 nm (204 bands). The camera employs a pushbroom line scanner and produces images with 512 × 512 pixels. Hyperspectral photographs were taken from six different zenith angles: −55°, −15°, 0°, 15°, 40° and 55°. The light source was a 12 V 50 W Quartz Tungsten Halogen lamp with a 36° beam. Negative angles are measured in the backward scattering (lamp) direction and positive angles in the forward scattering direction. All photographs were taken in the lamp principal plane so the azimuth angle was the same for all measurements. The illumination zenith angle was −40°. The measurement setup is illustrated in Fig. A1 in the Appendix.

The samples were allowed to dry indoors for a week before the measurements, i.e. no "fresh" samples were measured with the camera. This is because lichens dry very quickly indoors, and even faster under the strong lamp used as an illumination source for the measurements. As the acquisition of the reflectance spectra in six different angles took ca. 25 min, the sample's moisture content during the course of the measurement would have changed significantly.

The biconical reflectance factor (hereafter reflectance) was calculated as:

$$R = \frac{I_s - I_{dc,s}}{I_{wr} - I_{dc,wr}} \times \frac{t_2}{t_1} \times R_{wr} \tag{2}$$

In addition to notation in Eq. (1), $I_{dc,s}$ and $I_{dc,wr}$ are the dark current readings for the measurements of the sample and white reference panel, respectively, and t_1 and t_2 are the integration times in milliseconds used to capture the sample and white reference, respectively. Contrary to spectrometer measurements, the integration times of the white reference and sample required a manual optimization when using the hyperspectral camera, which caused the difference between Eqs. (1) and (2).

The pixels used in the final analysis were selected using manually created rectangular masks. The masks were created separately for every image and angle by selecting the area with the strongest illumination (using the image of the white reference panel) and checking the sample position within this area (using the image of the sample). The average masked area was 34,000 pixels. Note that the variation in illumination level has been accounted for by calculating the pixelwise reflectance values using both pixelwise values of sample and white reference measurements. Wavelengths outside the range 415–925 nm (i.e. 400–415 nm and 925–1000) were left out from the analysis due to

unstable reflectance values in these regions (Behmann et al., 2018).

2.3. Analysis of spectrometer measured spectra

Spectra of fresh and dry lichen samples were compared by employing a *t*-test to identify wavelengths in which the spectra of fresh and dry samples differ, and a one-directional variance test to test whether the variance in reflectance was higher for fresh than for dry samples. In the following analyses, only dry samples were used.

In order to evaluate interspecific differences in the shape of the spectra, the species-specific mean spectra of the dry samples were normalized so that the area under each spectrum equaled to 1.

Principal component analysis (PCA) was used to visualize the spectral variation of samples of different species, as well as to gain input data for a clustering analysis. Next, we employed a hierarchical clustering analysis to study the grouping of the samples based on their spectral information (e.g. Rees et al., 2004; Roth et al., 2016). The algorithm starts by assigning each observation to its own cluster and continues with merging the clusters closest in the distance space, finally forming a cluster tree. The Ward agglomerative hierarchical clustering method with squared Euclidean distances was used (Murtagh and Legendre, 2014). To avoid problems caused by high dimensional data, i.e. too many variables if all 2151 spectral bands were used, (e.g. Berkhin, 2006), the scores of the first three principal components for each sample were used in the clustering analysis.

To analyze variation in spectra between lichen species, we computed spectral angles in radians (e.g. Kruse et al., 1993) between species-specific mean dry spectra at certain wavelength regions.

To illustrate the interspecific variability in lichen reflectance from a practical remote sensing perspective, the species-specific mean fresh and dry spectra were resampled to the ten Sentinel-2 bands with 10 m or 20 m spatial resolution.

All the analyses were performed using the R software.

2.4. Analysis of multiangular spectra

Mean spectral reflectance values were computed for each sample and further, for each species, in order to compare the species-specific directional reflectance values. Anisotropy factors (Sandmeir and Itten, 1999) were computed for the species-specific mean reflectance values at each wavelength by dividing the reflectance at all other viewing angles by reflectance at nadir.

Spatial variation in reflectance within the lichen samples was quantified by calculating coefficients of variation (sample standard deviation divided by the mean) and by plotting kernel density plots for all pixels of selected wavelengths of one sample per species. The sample was systematically selected so that it was the first sample of each species that was measured. The results are shown for four wavelengths which coincide with Sentinel-2 bands in the visible-near-infrared range (490, 560, 664 and 841 nm).

3. Results

3.1. Spectrometer measurements

The general shape of the mean reflectance spectra was quite similar for all species, yet the brightness of reflectance varied both between and within species (Fig. 1). For both fresh and dry samples, *Cladonia stellaris* had the highest reflectance in the visible (VIS, 400–700 nm), near-infrared (NIR, 700–1300 nm) and shortwave infrared (SWIR, 1300–2500 nm) regions, followed by *Cladonia arbuscula*. In VIS, *Cladonia gracilis* subsp. *gracilis*, *Cladonia gracilis* subsp. *turbinata*, *Cladonia crispata*, *Cladonia phyllophora*, *Cladonia cornuta* as well as *Cetraria islandica* showed the lowest reflectance, whereas in NIR and SWIR, *Cladonia gracilis* subsp. *gracilis*, *Cladonia gracilis* subsp. *turbinata*, *Cladonia crispata*, *Cladonia phyllophora*, *Cladonia cornuta* and *Stereocaulon* species

had generally the lowest reflectance. The shape of the species-specific mean spectra varied most in the ultraviolet (UV, 350–400 nm) and VIS wavelength ranges: At wavelengths ca. 350–390 nm, the rapid increase in reflectance observed for *Stereocaulon tomentosum*, *Stereocaulon saxatile* and *Cladonia rangiferina* was clearly distinguishable from the shape of the spectra of the other species. In addition, the increase in reflectance in the green-yellow (maximum at 560 nm), as well as decrease in reflectance in the chlorophyll absorption area in the red (minimum at 680 nm) were weaker for *Cladonia gracilis* subsp. *gracilis*, *Cladonia gracilis* subps. *turbinata*, *Cladonia crispata*, *Cladonia cornuta* as well as *Cetraria islandica* than for other species. Additionally, the increase in reflectance in the beginning of the NIR region was more gradual for these species than for the other species. The normalization of the species-specific mean spectra of dry samples (Fig. 1e) indicated a relatively high reflectance in VIS and low in SWIR for *Cladonia stellaris*, *Cladonia arbuscula* and *Cladonia uncialis*, whereas *Cladonia gracilis* subsp. *gracilis*, *Cladonia gracilis* subps. *turbinata*, *Cladonia crispata*, *Cladonia phyllophora* and *Cladonia cornuta* showed relatively low reflectance in VIS and high in SWIR. *Cladonia uncialis* had a relatively high reflectance in the first half and *Cetraria islandica* in the second half of the NIR region.

Reflectance in the SWIR region was statistically significantly higher for dry than for fresh samples (Fig. 2), whereas in the NIR and VIS regions the differences between fresh and dry samples varied between species and were often not statistically significant (Fig. 2). The variance tests showed that for *Cetraria islandica*, *Cladonia arbuscula, Cladonia crispata, Cladonia gracilis* subsp. *gracilis* and *turbinata, Cladonia phyllophora, Cladonia rangiferina, Cladonia uncialis* and *Stereocaulon saxatile*, the variance in reflectance was not higher for the fresh than for the dry samples at any wavelength at 5% significance level, while for *Cladonia stellaris*, the variance was higher for fresh samples at wavelengths above 2448 nm, for *Stereocaulon tomentosum* at wavelengths 370–400 nm and 716–1350 nm and for *Cladonia cornuta* at wavelengths 353–404 nm. To provide reference values for future studies in remote sensing of lichens, we also report how the species-specific fresh and dry mean reflectances would have differed in typical multispectral satellite data (i.e., in this case resampled to Sentinel-2 bands) (Table A1 in the Appendix).

The first three principal components explained 97% of the variance in the reflectance spectra of the dry samples (PC1 87%, PC2 6% and PC3 4%). The projection of lichen samples onto the first and second, and first and third principal components visualizes the spectral differences between samples and species (Fig. 3). Samples of different species were arranged in overlapping groups, except for samples of *Cladonia uncialis* and *Cetraria islandica*, which formed distinct groups along the second and third principal components, respectively. *Cladonia gracilis* subsp. *gracilis*, *Cladonia gracilis* subps. *turbinata*, *Cladonia crispata*, *Cladonia phyllophora* and *Cladonia cornuta* arranged close to each other at the other end of the first principal component. *Cladonia stellaris*, *Cladonia arbuscula* and *Cladonia rangiferina,* on the other hand, were best separated from each other by the second principal component.

The first three principal components were used as input variables in the hierarchical clustering analysis. Similar patterns in spectral differentiation of samples and species were observed as in the PCA: If six clusters were chosen (rectangles surrounded by a dotted line, Fig. 4), *Cladonia uncialis* and *Cetraria islandica* clustered in their own, species-specific clusters. Nine of ten *Cladonia stellaris* samples were found in the same cluster, whereas *Cladonia arbuscula* samples were mixed with samples of *Cladonia stellaris*, *Cladonia rangiferina* and *Stereocaulon saxatile*. All *Stereocaulon tomentosum* samples were assigned into the same cluster, although with *Stereocaulon saxatile, Cladonia rangiferina, Cladonia gracilis* subsp. *gracilis*, *Cladonia gracilis* subps. *turbinata*, *Cladonia crispata*, *Cladonia phyllophora* and *Cladonia cornuta*. *Cladonia gracilis* subsp. *gracilis*, *Cladonia gracilis* subps. *turbinata*, *Cladonia crispata*, *Cladonia phyllophora* and *Cladonia cornuta* were found in two adjacent clusters.

The spectral angles (in radians) computed between species-specific mean spectra were highest in the UV region, followed by VIS, NIR and
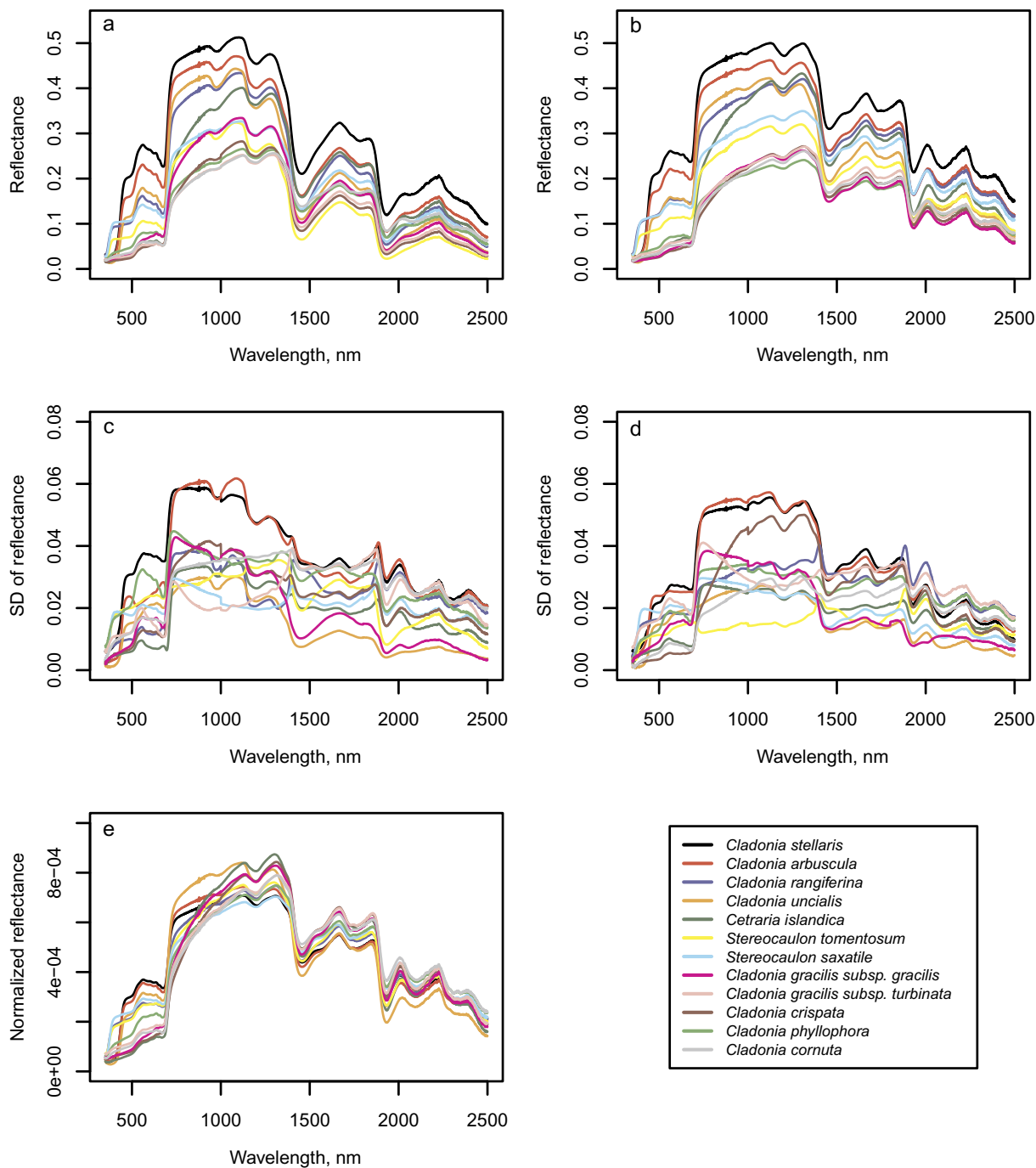
Fig. 1. Species-specific mean reflectance spectra of a) fresh samples and b) dry samples, standard deviations (SD) of reflectance spectra of c) fresh samples and d) dry samples, and e) normalized reflectance spectra of dry samples measured with a spectrometer.

SWIR regions (Fig. 5). The larger the angle between the spectra, the more different they are. *Stereocaulon saxatile, Stereocaulon tomentosum* and *Cladonia rangiferina* deviated the most from other species in the UV region. On the other hand, the results underline the spectral similarity of 1) *Cladonia stellaris* and *Cladonia arbuscula*, 2) *Stereocaulon tomentosum, Stereocaulon saxatile, Cladonia rangiferina* and perhaps *Cladonia gracilis* subsp. *gracilis*, and 3) *Cladonia gracilis* subsp. *gracilis*, *Cladonia gracilis* subps. *turbinata, Cladonia crispata, Cladonia phyllophora* and *Cladonia cornuta*.

3.2. Multiangular measurements with a hyperspectral camera

Reflectance of all lichen species was highest in the backscattering direction and lowest in the forward scattering direction in all wavelengths (Fig. 6). The deviation in brightness between samples of some species was high (Fig. 6) as was noticed also for the spectrometer measurements. For *Cetraria islandica*, the reflectance in backscattering directions (−55° and − 15°) was higher in relation to reflectance at nadir than for other species, i.e. the anisotropy factor was higher especially in the visible wavelengths (Fig. 7). In other view angles the anisotropy factors were similar across species (Fig. 7). The backscattering enhancement in reflectance was slightly higher for VIS than for NIR wavelengths, whereas in forward scattering directions the reflectance was slightly higher in NIR than in VIS in relation to that in nadir direction (Fig. 7).

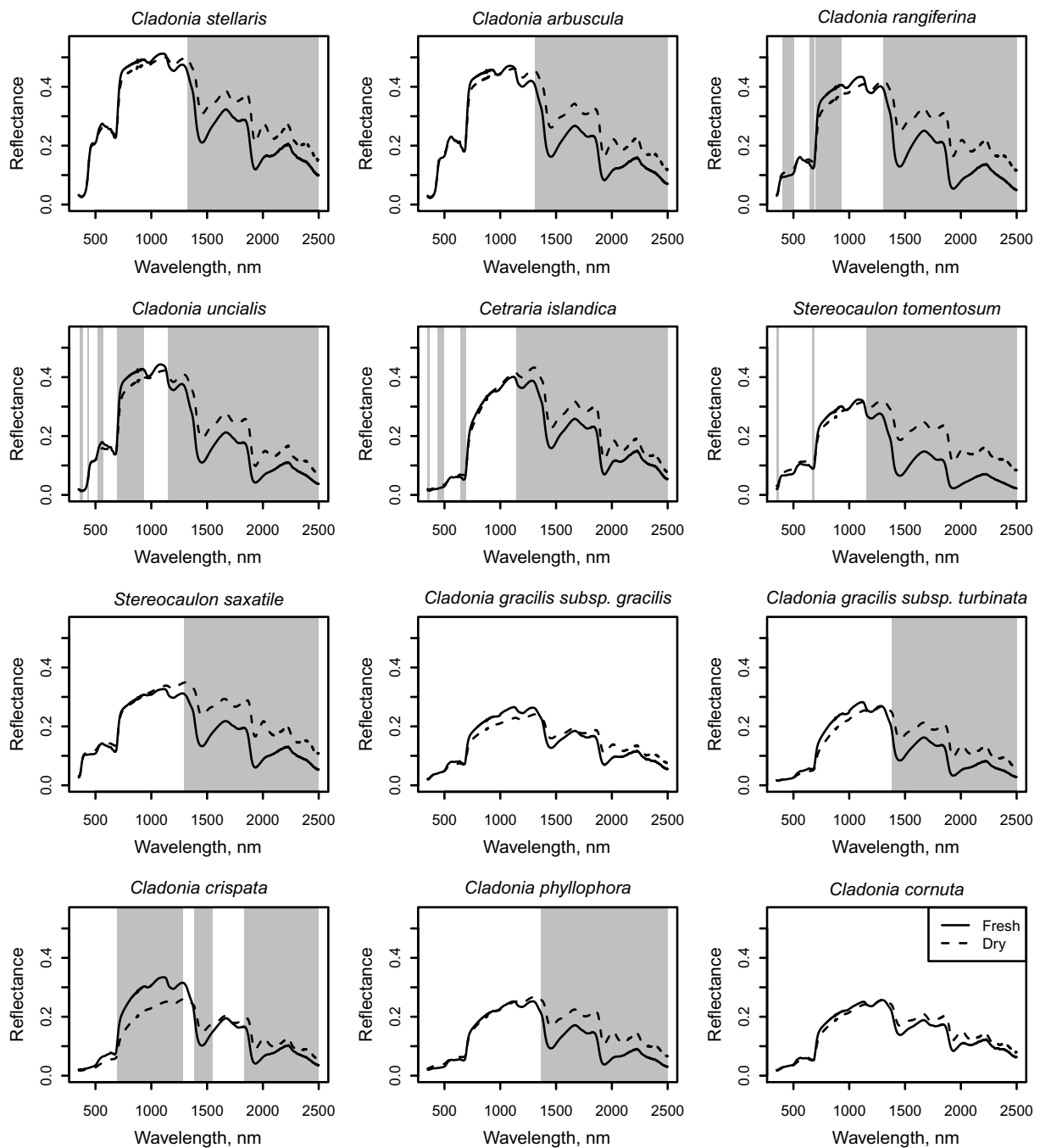The spatial variation of reflectance within lichen samples is

Fig. 2. Mean reflectance spectra of the fresh and dry samples of each species measured with a spectrometer. Grey areas denote wavelength regions with statistically significant (at 5% significance level) difference between fresh and dry samples.

illustrated by kernel density plots estimated using reflectance values of all image pixels at specific wavelengths for one sample of each species (Fig. 8). The density plots estimated for other samples of the same species were similar to those seen in Fig. 8. The estimated coefficients of variation revealed that the variation in reflectance relative to the mean was higher in VIS than in NIR for all species, and that the variation was higher in the nadir and forward scattering directions compared to backward scattering direction for all species (Fig. 8).

4. Discussion

4.1. Intraspecific variation in lichen spectra

Variation in reflectance between samples of a single species was often large, which emphasizes the need to measure several samples of each lichen species when quantifying their spectral properties. Variation in reflectance spectra within lichen species could be caused by, at least, structural variation in the lichen samples, variation in concentration of lichen substances, variation in sample water content, or varying type or amount of litter on the bottom of the samples.

Lichen substances are secondary compounds, usually phenolic acids, produced by the mycobiont. These substances have several roles in
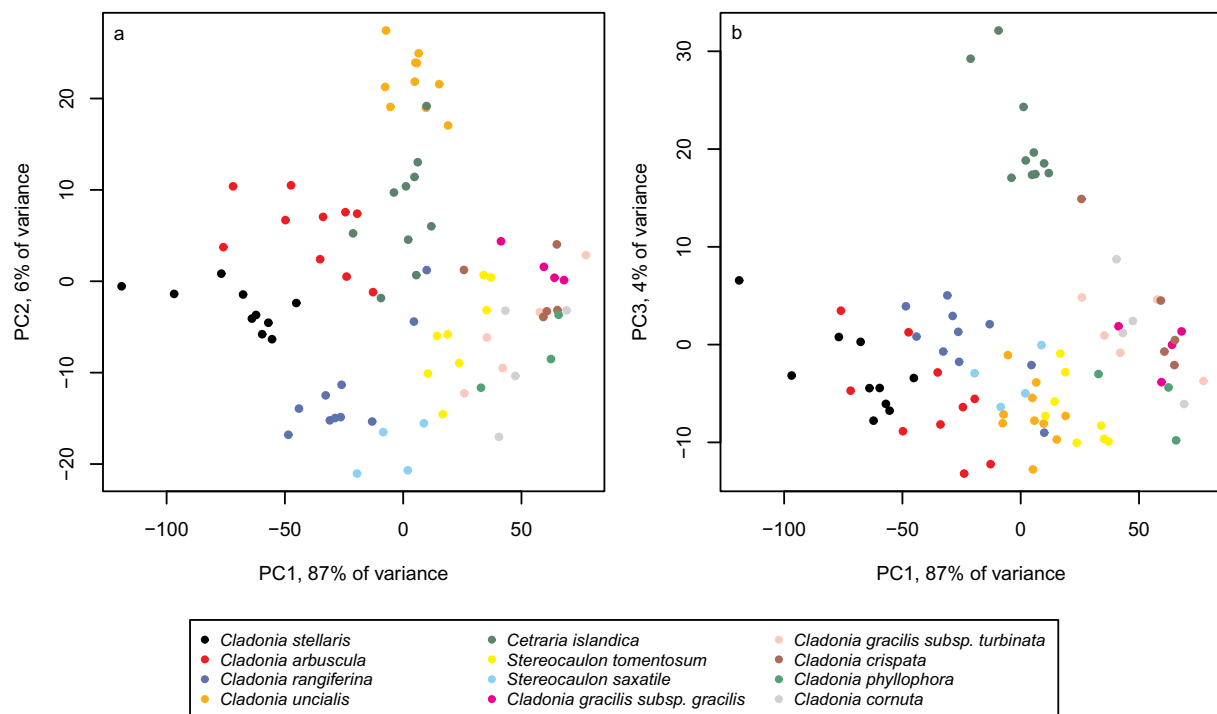
Fig. 3. Projection of samples onto the first and second (a), and first and third (b), principal components, and the percentages of the total variance explained by each component.

lichen protection (e.g. Asplund and Wardle, 2017), and some of these substances, mainly those occurring in the upper cortex/surface, have been observed to absorb or reflect UV and sometimes PAR (photo-synthetically active radiation) to protect the photobiont cells from excess solar radiation (e.g. McEvoy et al., 2007; Solhaug et al., 2010). McEvoy et al. (2007) observed the total thallus concentration of pho-toprotective usnic acid (which is also present in three of our study species: *Cladonia arbuscula*, *Cladonia stellaris*, and *Cladonia uncialis*) in *Nephroma arcticum* to increase from shaded habitats to open ones, at the same time as the transmittance of the cortical layer to UV and PAR decreased. They also observed the cortex thickness of the studied lichen to vary between habitats. Therefore, growth environment could have an influence on the intraspecific differences in spectra through changes in contents of secondary compounds and lichen structure.

Some of the measured species have naturally a large variation in structure. For example, the individual thalli of *Cladonia stellaris* can be loosely or tightly attached to each other, which influences the amount and depth of shadow within the sample. Indeed, we observed correlations between the "non-shadow fraction" (estimated using automatic thresholding of an image analysis software, not shown) and reflectance in wavebands of green, blue, red, NIR and SWIR regions (Pearson's correlation coefficient 0.19 at 490 nm, 0.36 at 560 nm, 0.24 at 665 nm, 0.53 at 842 nm, 0.50 at 1610 nm and 0.47 at 2190 nm). A corresponding analysis was conducted also for *Cladonia rangiferina*, and the correlations were 0.48 at 490 nm, 0.51 at 560 nm, 0.43 at 665 nm, 0.56 at 842 nm, 0.22 at 1610 nm and 0.12 at 2190 nm.

The reflectance of fresh lichen samples was usually similar to that of dry samples in VIS, similar or slightly higher in NIR and lower in SWIR. These results are comparable to those of Granlund et al. (2018), Nordberg and Allard (2002) and Neta et al. (2010). Rees et al. (2004) observed lower reflectance of wet samples compared to dry samples of several lichen species in all wavelengths, except for *Cladonia arbuscula*, for which the reflectance of a wet sample was lower than that of a dry sample only in the SWIR region and for a *Stereocaulon* species, for which the reflectance of a wet sample was higher compared to a dry sample in all wavelengths. The differences in reflectance between fresh and dry

lichen in VIS and NIR varies between and within studies, but all agree that the reflectance of fresh samples is generally lower than that of dry samples in the SWIR region with water absorption. However, it must be noted that two days of drying may not have dried the samples completely, and some of the intraspecific variation in reflectance of the dry samples (in SWIR) may still be caused by differences in moisture content.

4.2. Interspecific differences in lichen spectra

Results of the clustering analysis suggested that some of the variation in lichen spectra could be related to taxonomical differences, or at least to differences in physical traits such as structure or chemical composition, that can be related to phylogenetic similarity. Only two species, *Cetraria islandica* and *Cladonia uncialis* formed their own species-specific clusters in the dendrogram (see center branches in Fig. 4). For the other species, the following reasoning can be provided to explain the multispecies clusters that they formed. One of the two main branches of the dendrogram (i.e., the lowest main branch in Fig. 4) almost solely consisted of samples of the *Cladonia* lichens belonging to three species (*Cladonia arbuscula*, *Cladonia stellaris* and *Cladonia rangiferina*). Most of the samples belonging to these species arranged in species-specific clusters, but there were some exceptions. These lichen species are phylogenetically not particularly closely related (Stenroos et al., 2019), but they have a similar richly branched growth habit, which may explain their spectral similarities. However, from the perspective of their biochemical composition, the pigment contents of *Cladonia stellaris* and *Cladonia arbuscula* are similar to each other, yet differ from those of *Cladonia rangiferina* (see discussion in 4.1. and 4.2.). In the other main branch of the dendrogram (i.e., in the upper main branch in Fig. 4), the clusters were clearly more heterogeneous in terms of the species that were included. In this branch of the dendrogram, *Cladonia* species (*Cladonia gracilis* subsp. *gracilis*, *Cladonia gracilis* subps. *turbinata*, *Cladonia crispata*, *Cladonia phyllophora* and *Cladonia cornuta*) were mixed with *Stereocaulon* species. A potential explanation for this is that *Cladonia gracilis* subsp. *gracilis*, *Cladonia gracilis* subps. *turbinata* and
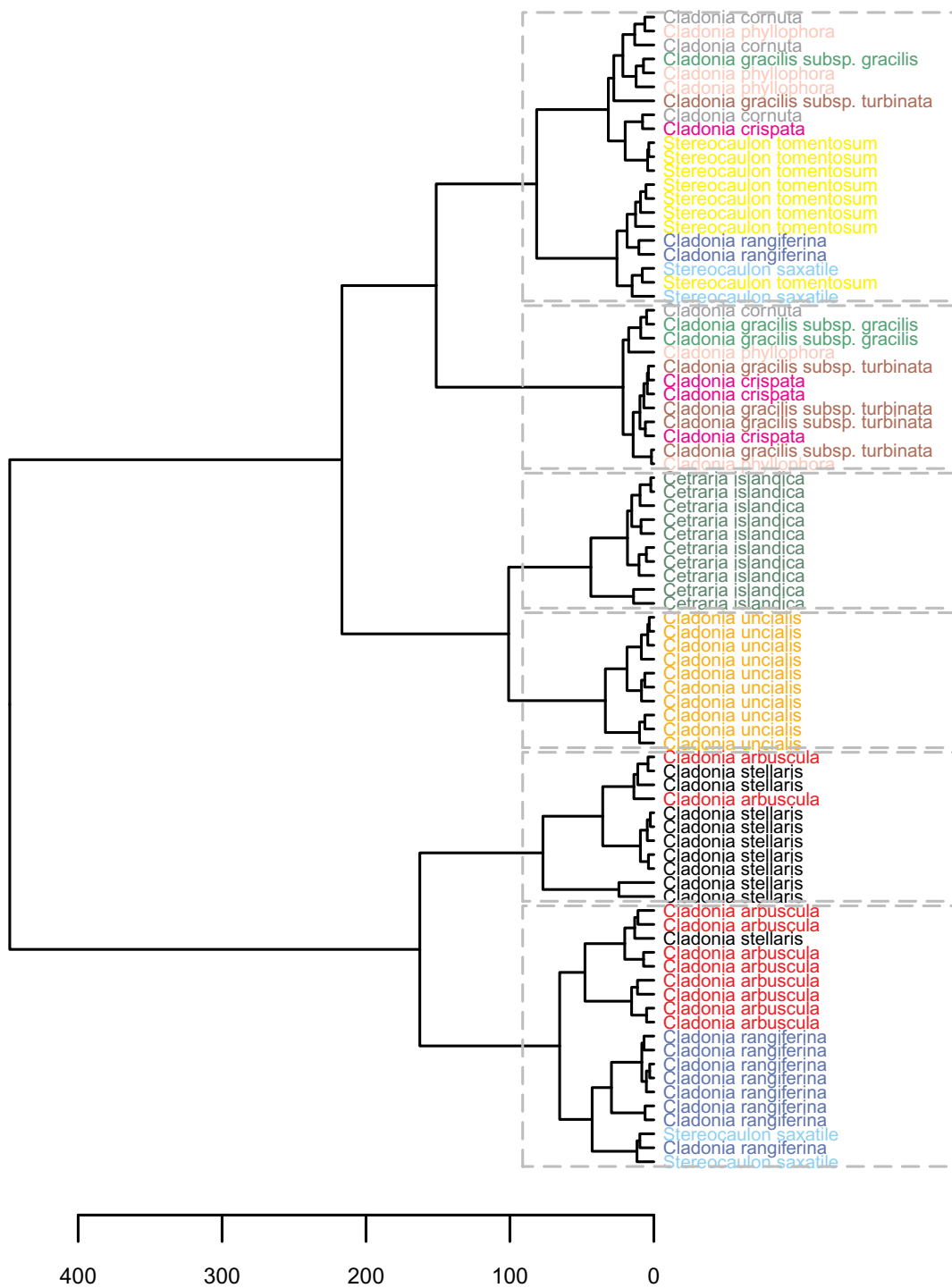
Fig. 4. Dendrogram produced by hierarchical clustering analysis. The rectangles denote clusters when the cluster number is set at 6.

Cladonia cornuta belong to the same *Graciles* subclade under the Cladoniaceae family, and that the family Stereocaulaceae is taxonomically closely related to the family Cladoniaceae (Stenroos et al., 2019).

As for the within-species differences, the occurrence and concentration of lichen substances probably has an influence also on the between-species differences in reflectance spectra. For example, Nelson et al. (2013) reported that lichens containing usnic acid are separable from remote sensing imagery due to their high reflectance in the blue-green region. Indeed, the species containing usnic acid (*Cladonia arbuscula*, *Cladonia stellaris* and *Cladonia uncialis*) had the highest reflectance in the blue-red range in this study. In addition to usnic acid,

atranorin is a compound that can be abundant in the cortical layer of some lichen species and is known to protect the photosynthesis of green algae by reflecting excess solar radiation (Solhaug et al., 2010). From the species presented in this study, atranorin is found in *Cladonia rangiferina*, *Stereocaulon saxatile* and *Stereocaulon tomentosum*. These species were observed to have a distinct increase in spectra in the UV-blue region. However, we do not know if these two facts are connected to each other, especially as Solhaug et al. (2010) observed that the reflectance of atranorin containing thallus was higher than that of the acetone-rinsed thallus throughout the VIS-NIR spectrum. They suspected this to be caused by Mie scattering of the atranorin crystals in
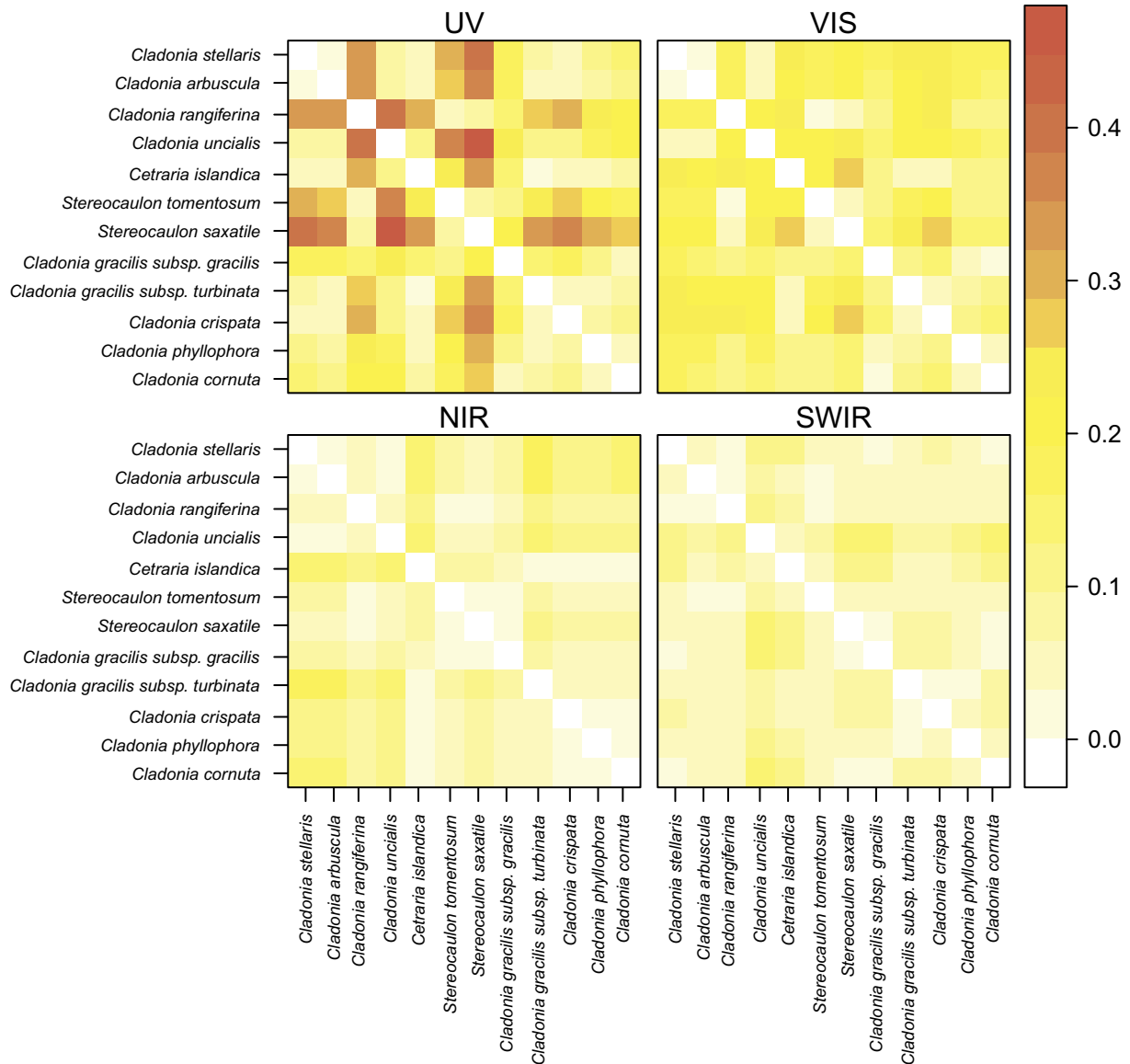
Fig. 5. Spectral angles in radians between mean spectra for each species.

the hyphal interphases.

Visually, the color of some *Cladonia* lichens (*Cladonia gracilis* subsp. *gracilis*, *Cladonia gracilis* subps. *turbinata*, *Cladonia crispata*, *Cladonia phyllophora* and *Cladonia cornuta*) turned rather dark as they dried, which might be related to a thick surface layer and partly explain their low reflectance in the visible wavelengths. Another reason could be the structure of these lichens, with usually a plenty of shadow viewed by the sensor between the individual thalli. The spectra of both *Stereocaulon* species (*S. saxatile* and *S. tomentosum*) resembled each other, but *Stereocaulon saxatile* had higher reflectance throughout the spectrum. The visual appearance of *Stereocaulon saxatile* is lighter and the growth type denser, which might explain some of the differences.

Simple reflectance ratios that could be used to separate lichen species or species groups would be helpful in identification of species from remote sensing data. Bechtel et al. (2002) measured spectral properties of one foliose and four crustose lichen species and proposed plotting spectral ratios of 400/685 nm against 773/685 nm for discrimination between lichen species. We also tried this and found that using these ratios we can get roughly four groups of species: 1) *Cladonia arbuscula, Cladonia stellaris, Cladonia uncialis*, 2) *Cetraria islandica*, 3) *Cladonia rangiferina, Stereocaulon saxatile, Stereocaulon tomentosum* and

4) *Cladonia gracilis* subsp. *gracilis*, *Cladonia gracilis* subps. *turbinata*, *Cladonia crispata, Cladonia phyllophora, Cladonia cornuta* (not shown). This grouping is largely caused by differences in the spectra at 400 nm. Based on the normalized spectra of dry samples (Fig. 1e), we suggest the following reflectance ratios for the separation of some lichen species or species groups (Fig. A14): *Cladonia uncialis* shows a comparatively low relative reflectance in the second half of the SWIR region and high relative reflectance in the first half of the NIR region, wherefore a ratio between reflectances (R) in wavelengths from these regions, such as R_{900nm}/R_{2020nm}, could be used to separate *Cladonia uncialis* from other species of this study. Similarly, the ratio of R_{550nm}/R_{1130nm} could be used to separate *Cladonia stellaris* and *Cladonia arbuscula* from other species, and the ratio of R_{1300nm}/R_{680nm} *Cetraria islandica*. *Cetraria islandica* could also be discriminated using derivative of the reflectance spectra in the beginning of the NIR region, e.g. $(R_{850nm}-R_{750nm})/100$. The ratio of e.g. R_{400nm}/R_{1670nm} could be used to separate *Cladonia rangiferina* and both *Stereocaulon* species from other studied species, but the similar shapes of the spectra of these species suggest that it may not be possible to separate them based on the shape of their spectra, but rather based on the higher reflectance of *Cladonia rangiferina* compared to *Stereocaulon* species (Fig. 1a–b). As a practical limitation, it is
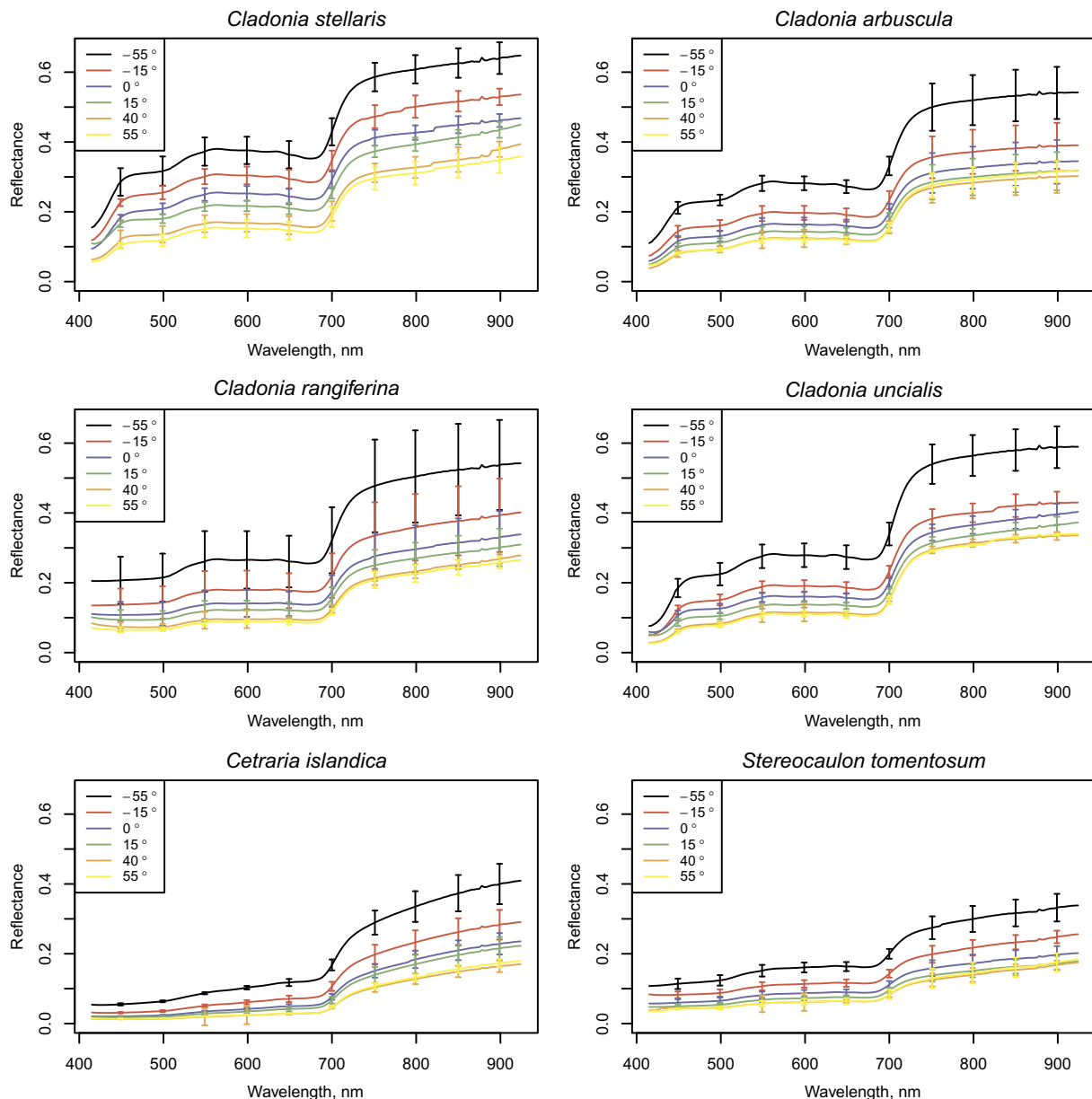
Fig. 6. Species-specific mean reflectance at different view zenith angles along the principal plane measured with a hyperspectral camera. Negative angles denote backscattering direction (lamp angle −40°), and positive angles forward scattering direction.

important to note that these indices apply only to spectra of dry lichens.

4.3. Directional reflectance properties of lichens

The coefficients of variation of within-sample reflectances were the highest in the nadir-view direction. This is logical since the variation in lighted and shaded areas in the lichen mat could be expected to be largest in this direction. Furthermore, the variation in reflectance in nadir- and forward-view was the largest for *Cetraria islandica*, which could be explained by the contrast between possible specular reflectance from the lobes of the "leaf-like" thalli and deep shadows under them. We observed a stronger backscattering enhancement for *Cetraria islandica* than for other measured species, but otherwise the differences between species were small. The measurement setup allowed us to measure the backscattering reflectance 15 and 25 degrees (i.e., at −55° and −15° in Fig. 6, respectively) away from the lamp zenith direction (−40°). Even though not very close to exact hotspot, the backscattering reflectance at −55° was clearly higher than reflectance at nadir (ca.

1.5–2.5 times higher, Fig. 7), or in forward scattering directions. These results are compatible with the results of Solheim et al. (2000), Kaasalainen and Rautiainen (2005), and Peltoniemi et al. (2005), who all measured high backscattering reflectances of two to several lichen species. Solheim et al. (2000) further observed that backscattering was higher for a higher zenith angle. Kaasalainen and Rautiainen (2005) suggested the strong scattering peak in the hotspot direction of "reindeer lichens" (richly branched *Cladonia*) to be caused by hiding of shadows of the structurally complex lichens in this direction. They demonstrated this phenomenon by measuring powdered lichen samples. Both Kaasalainen and Rautiainen (2005) and Solheim et al. (2000) acknowledged the distinctive directionality of lichens' reflectance to benefit their recognition from remote sensing data. However, based on this or previous studies, it is still difficult to conclude whether information on lichen targets' directional reflectance properties would help to identify lichen species.
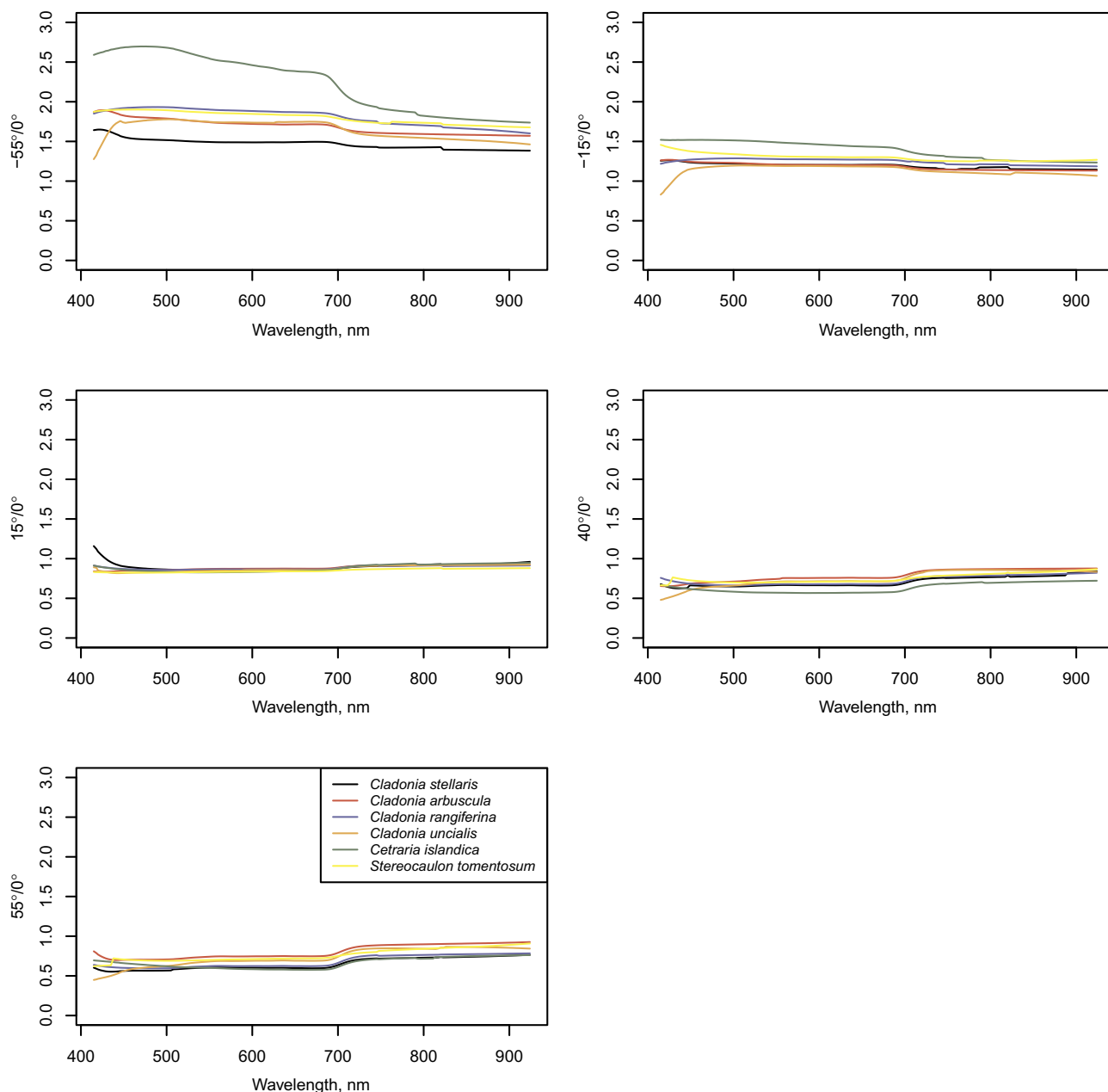
Fig. 7. Species-specific average anisotropy factors for the angles measured using a hyperspectral camera.

4.4. Remote sensing applications

The use of spectral data collected by drones, in addition to satellite imagery, has recently gained attention in monitoring changes occurring in remote, high-latitude vegetation and soil crust communities (including lichens) (Myers-Smith et al., 2020). In the boreal and tundra regions, lichens typically grow in open areas (where flying drones low is possible) and in sparse forests (where the visibility of ground to a sensor on the drone is tolerable). Therefore, it is possible to obtain very high-spatial resolution spectral data of lichen mats in many situations, and potentially to use it to map at least some lichen species. In general, our results indicate that narrow-band spectral reflectance data would be needed if identification of ground lichen species is attempted. Some of the lichen species measured in this study, at least *Cladonia arbuscula*, *Cladonia stellaris*, *Cladonia rangiferina*, *Cladonia uncialis* and *Cetraria is-landica*, may cover large areas of ground in the boreal region. Our results indicate that the measured spectra could be applied for

identification of lichens using e.g. spectral mixture analysis methods. Some of the species, on the other hand, only grow as small assemblages, wherefore their identification from even drone images may not be realistic due to the mismatch of spatial resolutions. This group includes *Cladonia gracilis* subsp. *gracilis*, *Cladonia gracilis* subps. *turbinata*, *Cladonia crispata*, *Cladonia phyllophora*, *Cladonia cornuta* and *Stereocaulon saxatile*. The identification of these lichens can, however, be difficult even in-situ based on traditional visual assessment. Perhaps their identification in field inventories could be improved in the future by close-range sensing using automated detection algorithms applied to spectral images obtained by mobile hyperspectral cameras. In addition to (pointwise) nadir-view spectra, our study indicates that the identification should probably be based on the variation in reflectance within the lichen mat, i.e. lichen surface structure which can be inferred from hyperspectral images (and not spectral point measurement data, as provided e.g., by the ASD instrument). This is particularly because the nadir-view spectra of species which are often difficult to identify (in this
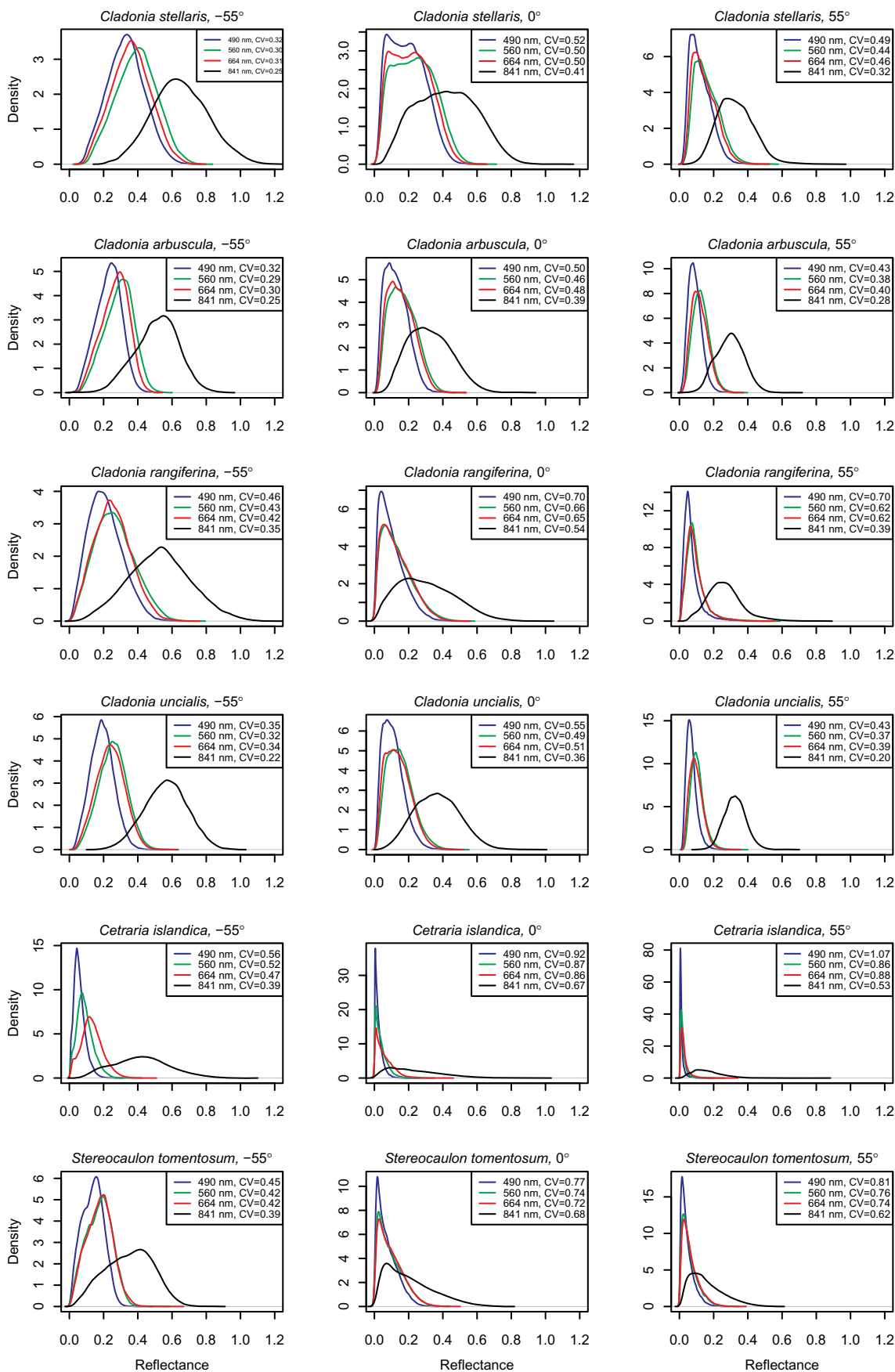
Fig. 8. Variation in within-sample reflectance in one sample of six lichen species, as measured by the hyperspectral camera, illustrated by kernel density plots estimated for all pixels of specific wavelengths (490, 560, 664 and 841 nm). CV denotes coefficient of variation.

case, *Cladonia gracilis* subsp. *gracilis*, *Cladonia gracilis* subps. *turbinata*, *Cladonia crispata*, *Cladonia phyllophora, Cladonia cornuta*) can be very similar. The use of surface structure (characterized by its spatio-spectral variation) as a classification tool would also diminish the problem of the effect of changing moisture content on lichens' reflectance. Such non-invasive methods based on spectral image data could offer a possibility also for non-experts to identify lichen species without removing and transporting samples for laboratory analyses.

5. Conclusions

This study showed that when spectral libraries of lichen species are established, the large intraspecific variation in lichen reflectance spectra and changes in their spectra due to the varying moisture content call for sampling strategies that take both of these effects into account. From the perspective of practical remote sensing, these variations will make the identification of lichen species from remote sensing data more complicated.

Our study indicated that some common boreal lichen species (e.g., *Cetraria islandica*, *Cladonia uncialis*) are spectrally different from others. However, this result may depend on the set of studied species; for example, in this case no other *Cetraria* species was measured. Some of the studied lichen species had, on the other hand, very similar nadir-view reflectance spectra, which can make their discrimination based on spectral properties difficult. Spectral similarities of lichen species are not always related to their phylogenetic relatedness but to e.g., their similar growth forms and chemical composition. Our study also demonstrated that the added-value of multi-angular spectral data in identifying lichen species is not yet clear, and needs further investigation. Overall, information on the lichens' reflectance spectra and its directional properties could also help to separate them from other land cover types in remotely sensed images.

The lichen spectra (350–2500 nm) measured in this study are publicly available through the SPECCHIO Spectral Information System under campaign "Boreal lichens". In the future, this data can have versatile uses: it can be applied to test methods for identifying common boreal lichen species from high spatial resolution remote sensing data collected by e.g., drones, or as input data to physically-based canopy reflectance models or land surface models (as part of climate modeling).

Declaration of Competing Interest

The authors declare that they have no known competing financial interests or personal relationships that could have appeared to influence the work reported in this paper.

Acknowledgements

Appendix A. Supplementary data

Supplementary data to this article can be found online at https://doi.org/10.1016/j.rse.2020.111955.

References

Asplund, J., Wardle, D.A., 2017. How lichens impact on terrestrial community and ecosystem properties. Biol. Rev. 92, 1720–1738.

Bechtel, R., Rivard, B., Sánchez-Azofeifa, A., 2002). Spectral properties of foliose and crustose lichens based on laboratory experiments. Remote Sensing of Environment 82, 389–396.

Behmann, J., Aceborn, K., Emin, D., Bennertz, S., Matsubara, S., Thomas, S., Bohnenkamp, D., Kuska, M.T., Jussila, J., Salo, H., Mahlein, A.-K., Rascher, U., 2018. Specim IQ: evaluation of a new, miniaturized handheld hyperspectral camera and its application for plant phenotyping and disease detection. Sensors 18, 441.

Berkhin, P., 2006. A survey of clustering data mining techniques. In: Kogan, J., Nicholas, C., Teboulle, M. (Eds.), Grouping Multidimensional Data. Springer, Berlin, Heidelberg.

Bobbink, R., Hicks, K., Galloway, J., Spranger, T., Alkemade, R., Ashmore, M., Bustamante, M., Cinderby, S., Davidson, E., Dentener, F., Emmett, B., Erisman, J.-W., Fenn, M., Gilliam, F., Nordin, A., Pardo, L., de Vries, W., 2010. Global assessment of nitrogen deposition effects on terrestrial plant diversity: a synthesis. Ecol. Appl. 20, 30–59.

Elmendorf, S.C., Henry, G.H.R., Hollister, R.D., et al., 2012. Plot-scale evidence of tundra vegetation change and links to recent summer warming. Nat. Clim. Chang. 2, 453–457.

Falldorf, T., Strand, O., Panzacchi, M., Tømmervik, H., 2014. Estimating lichen volume and reindeer winter pasture quality from Landsat imagery. Remote Sens. Environ. 140, 573–579.

Granlund, L., Keski-Saari, S., Kumpula, T., Oksanen, E., Keinänen, M., 2018. Imaging lichen water content with visible to mid-wave infrared (400-5500 nm) spectroscopy. Remote Sens. Environ. 216, 201–310.

Hovi, A., Raitio, P., Rautiainen, M., 2017. A spectral analysis of 25 boreal tree species. Silva Fennica 51 (4), 7753.

Jääskeläinen, A., 2011. Suomen jäkälien uhanalaisuus. In: Stenroos, S., Ahti, T., Lohtander, K., Myllys, L. (Eds.), Suomen jäkäläopas. 29 Norrlinia 21.

Juola, J., 2019. Multi-Angular Measurement of Woody Tree Structures with Mobile Hyperspectral Camera. Aalto University, Master's thesis.

Kaasalainen, S., Rautiainen, M., 2005. Hot spot reflectance signatures of common boreal lichens. J. Geophys. Res. 110, D20102.

Käyhkö, J., Pellikka, P., 1994. Remote sensing of the impact of reindeer grazing on vegetation in northern Fennoscandia using SPOT XS data. Polar Res. 13, 115–124.

Keim, J.L., DeWitt, P.D., Fitzpatrick, J.J., Jenni, N.S., 2016. Estimating plant abundance using inflated beta distributions: applied learnings from a lichen–caribou ecosystem. Ecol. Evol. 7, 486–493.

Kruse, F.A., Lefkoff, A.B., Boardman, J.W., Heidebrecht, K.B., Shapiro, A.T., Barloon, J.P., Goetz, A.F.H., 1993. The spectral image processing system (SIPS) interactive visualization and analysis of imaging spectrometer data. Remote Sens. Environ. 44, 145–163.

McEvoy, M., Solhaug, K.A., Gauslaa, Y., 2007. Solar radiation screening in usnic acid-containing cortices of the lichen *Nephroma arcticum*. Symbiosis 43, 143–150.

Miadlikowska, J., Kauff, F., Högnabba, F., Oliver, J.C., Molnár, K., et al., 2014. A multigene phylogenetic synthesis for the class Lecanoromycetes (Ascomycota): 1307 fungi representing 1139 infrageneric taxa, 317 genera and 66 families. Mol. Phylogenet. Evol. 79, 132–168.

Murtagh, F., Legendre, P., 2014. Ward's hierarchical agglomerative clustering method: which algorithms implement Ward's criterion? J. Classif. 31, 274–295.

Myers-Smith, I.H., Kerby, J.T., Phoenix, G.K., Bjerke, J.W., Epstein, H.E., et al., 2020. Complexity revealed in the greening of the Arctic. Nat. Clim. Chang. 10, 106–117.

Nash, T.H., 2008. Lichen biology. Cambridge University Press, Cambridge.

Nelson, P.R., Roland, C., Macander, M.J., McCune, B., 2013. Detecting continuous lichen abundance for mapping winter caribou forage at landscape spatial scales. Remote Sens. Environ. 137, 43–54.

Neta, T., Cheng, Q., Bello, R.L., Hu, B., 2010. Lichens and mosses moisture content assessment through high-spectral resolution remote sensing technology: a case study of the Hudson Bay Lowlands, Canada. Hydrol. Process. 24, 2617–2628.

Nordberg, M.-L., Allard, A., 2002. A remote sensing methodology for monitoring lichen cover. Can. J. Remote. Sens. 28, 262–274.

Peltoniemi, J.I., Kaasalainen, S., Näränen, J., Rautiainen, M., Stenberg, P., Smolander, H., Smolander, S., Voipio, P., 2005. BRDF measurement of understory vegetation in pine forests: dwarf shrubs, lichen, and moss. Remote Sens. Environ. 94, 343–354.

Petzold, D.E., Goward, S.N., 1988. Reflectance spectra of subarctic lichens. Remote Sens. Environ. 24, 481–492.

Rees, W.G., Tutubalina, O.V., Golubeva, E.I., 2004. Reflectance spectra of subarctic lichens between 400 and 2400 nm. Remote Sens. Environ. 90, 281–291.

Roth, K.L., Casas, A., Huesca, M., Ustin, S.L., Alsina, M.M., Mathews, S.A., Whiting, M.L., 2016. Leaf spectral clusters as potential optical leaf functional types within California ecosystems. Remote Sens. Environ. 184, 229–246.

Sandmeir, S., Itten, K., 1999. A field goniometer system (FIGOS) for acquisition of hyperspectral BRDF data. IEEE Trans. Geosci. Remote Sens. 37, 648–658.

Schaepman-Strub, G., Schaepman, M.E., Painter, T.H., Dangel, S., Martonchik, J.V., 2006. Reflectance quantities in optical remote sensing—definitions and case studies. Remote Sens. Environ. 103, 27–42.

Solhaug, K.A., Larsson, P., Gauslaa, Y., 2010. Light screening in lichen cortices can be quantified by chlorophyll fluorescence techniques for both reflecting and absorbing pigments. Planta 231, 1003–1011.

Solheim, I., Engelsen, O., Hosgood, B., Andreoli, G., 2000. Measurement and modeling of the spectral and directional reflection properties of lichen and moss canopies. Remote Sens. Environ. 72, 78–94.

Stenroos, S., 2011. Jäkälien taksonomia. In: Stenroos, S., Ahti, T., Lohtander, K., Myllys, L. (Eds.), Suomen jäkäläopas: 29. Norrlinia 21.

Stenroos, S., Pino-Bodas, R., Hyvönen, J., Lumbsch, H.T., Ahti, T., 2019. Phylogeny of the family Cladoniaceae (Lecanoromycetes, Ascomycota) based on sequences of multiple loci. Cladistics 35, 351–384.

Stoy, P.C., Street, L.E., Jonhson, A.V., Prieto-Blanco, A., Ewing, S.A., 2012. Temperature, heat flux, and reflectance of common subarctic mosses and lichens under field conditions: might changes to community composition impact climate-relevant surface fluxes? Arct. Antarct. Alp. Res. 44, 500–508.

Thèau, J., Peddle, D.R., Duguay, C.R., 2005. Mapping lichen in a caribou habitat of northern Quebec, Canada, using an enhancement-classification method and spectral mixture analysis. Remote Sens. Environ. 94, 232–243.